Kumar et al., http://www.jcb.org/cgi/content/full/jcb.201404147/DC1

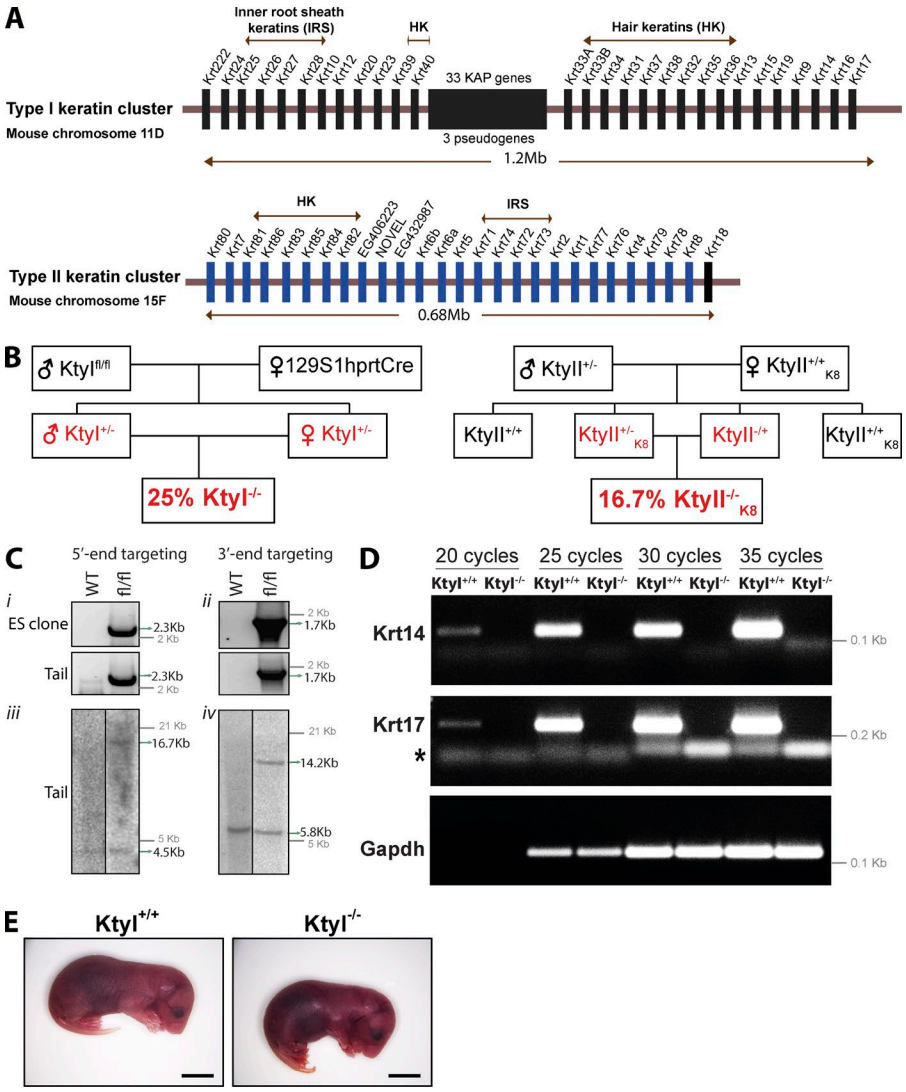

Figure S1. **Organization of keratin gene clusters and verification of keratin gene deletion.** (A) Representation of Ktyl and KtyII keratin gene cluster arrangement on mouse chromosomes 11 and 15, respectively. Note presence of type I keratin Krt18 on the extremity of KtyII cluster. HK, hair keratin; IRS, inner root sheath keratins; KAP, keratin-associated protein-coding genes. 1.2 and 0.68 Mb indicate size of keratin gene clusters, respectively. (B) Representation of mating strategy used for generating Ktyl$^{-/-}$ and KtyII$^{-/-}{}_{K8}$ mice. (C, i and ii) PCR identifying the floxed allele at 3′ and 5′ end of Ktyl mice and ES cells. (iii and iv) Southern blot showing homozygous floxed alleles at 3′ and 5′ end of Ktyl mice. (D) Semi-quantitative PCR performed from Ktyl$^{+/+}$ and Ktyl$^{-/-}$ keratinocytes showing the absence of type I keratins Krt14 and Krt17. GAPDH was used as internal control. Asterisk below Krt17 represents position of unspecific amplicon. (E) Phenotypic appearance of Ktyl$^{+/+}$ and Ktyl$^{-/-}$ E18.5 embryos. Bars, 5 mm.

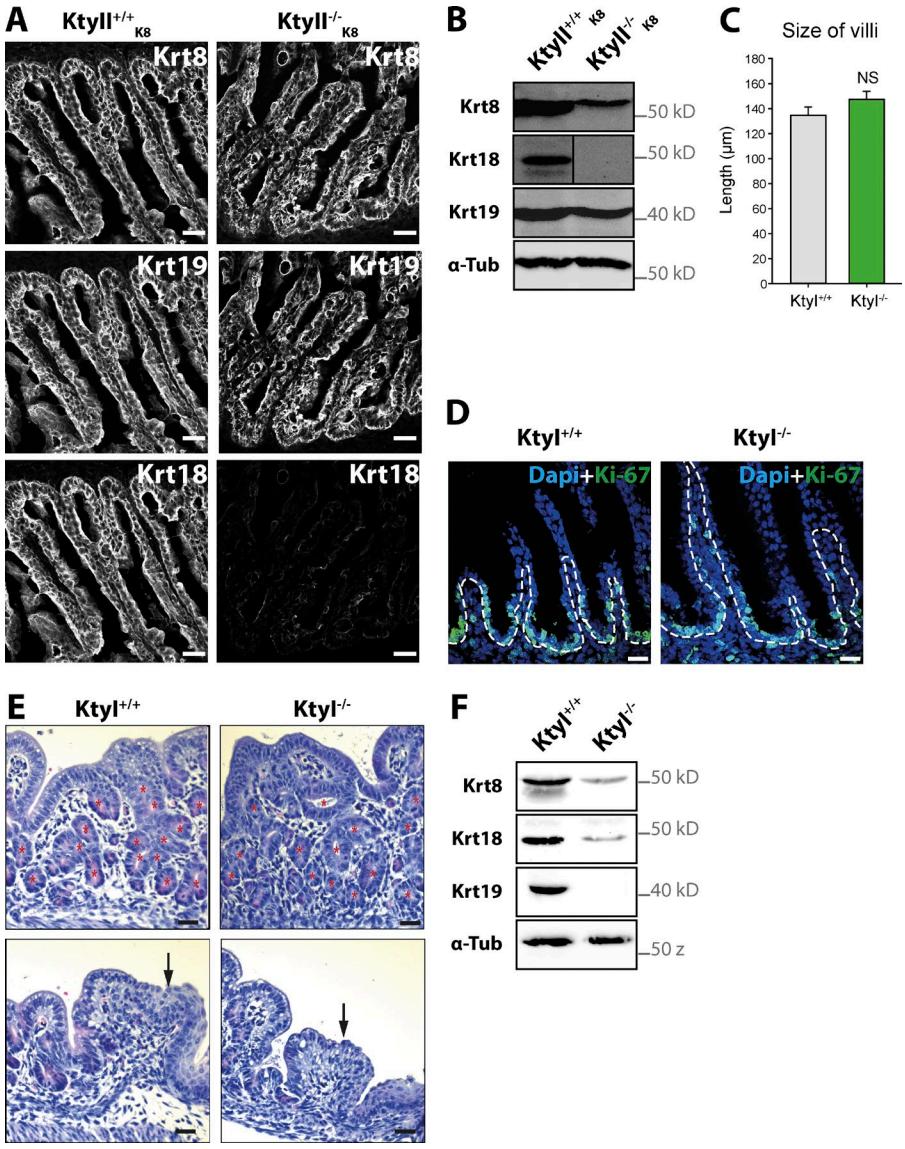

Figure S2. **Keratin expression pattern in intestine of Ktyll$^{+/+}{}_{K8}$ and Ktyll$^{-/-}{}_{K8}$ and analysis of Ktyl$^{+/+}$ and Ktyl$^{-/-}$ stomach.** (A) Immunofluorescence analysis of Krt8, Krt18, and Krt19 localization in intestines of Ktyll$^{+/+}{}_{K8}$ and Ktyll$^{-/-}{}_{K8}$ E18.5 embryos. Bars, 20 µm. (B) Western blotting of Krt8, Krt18, Krt19, and α-tubulin as loading control from intestines of Ktyll$^{+/+}{}_{K8}$ and Ktyll$^{-/-}{}_{K8}$ E18.5 embryos. (C) Microscopic measurement of the length of the villi in Ktyl$^{+/+}$ and Ktyl$^{-/-}$ intestine. (D) Immunofluorescence labeling of Ki-67 (green) and nuclei (blue) in the intestine of Ktyl E18.5 embryos. The basement membrane is represented by dotted lines according to a Krt8 staining. Bars, 10 µm. The percentage of proliferative epithelial cells (Ki-67 positive) is presented in D. (E) Hematoxylin/eosin-stained sections of stomach from E18.5 Ktyl$^{+/+}$ and Ktyl$^{-/-}$ embryos. Asterisks in red indicate the gastric gland of stomach. Black arrows projecting downward indicate the transition from forestomach to stomach. The dotted box in the intestine shows the magnified version in the black box. No lesions were detected in the Ktyl$^{-/-}$ intestine with cell shape, size, and number of enterocytes appearing unaltered. The mean length of intestinal villi is comparable in Ktyl$^{+/+}$ and Ktyl$^{-/-}$. Bars, 20 µm. Periodic acid–Schiff staining (bottom) of the stomach to identify goblet cells shows similar setting in E18.5 Ktyl$^{+/+}$ and Ktyl$^{-/-}$ embryos. Bars, 5 µm. (F) Same as B in Ktyl$^{+/+}$ and Ktyl$^{-/-}$ stomachs.

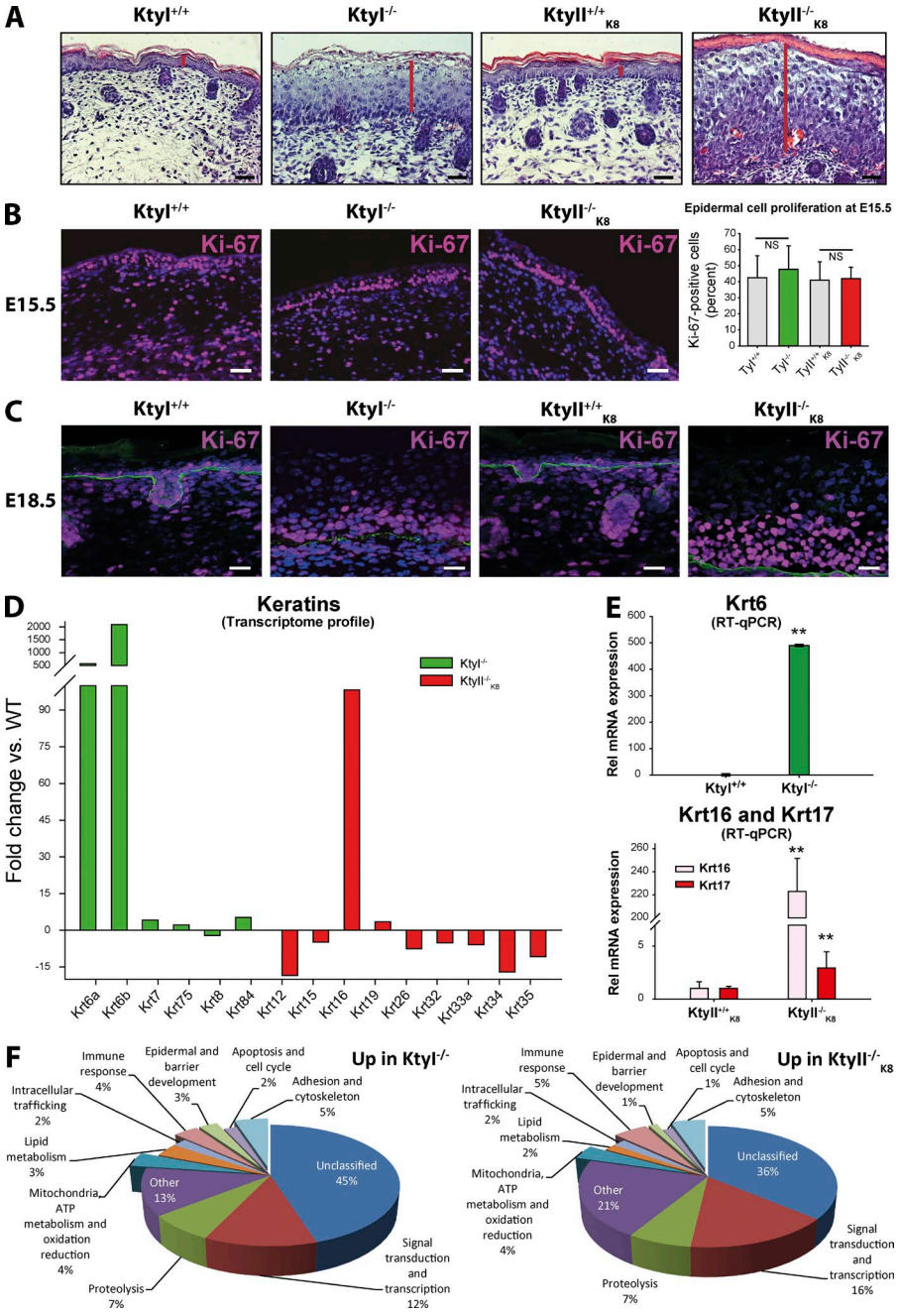

Figure S3. **Keratin-deficient skin histology, proliferation, and transcriptome profiling at E18.5.** (A) Hematoxylin/eosin-stained skin sections (see higher magnification of other pictures in Fig. 2 A); vertical red lines mark epidermal thickness. Bars, 20 µm. (B) Immunofluorescence staining and quantification of the percentage of Ki-67–positive cells (purple) among total cells (DAPI, blue) in WT and Ktyl$^{-/-}$ and Ktyll$^{-/-}{}_{K8}$ epidermis at E15.5. Bars, 30 µm. (C) Immunofluorescence staining of Ki-67 and β4-integrin (green) in WT and Ktyl$^{-/-}$ and Ktyll$^{-/-}{}_{K8}$ epidermis at E18.5. Percentages of Ki-67–positive cells are indicated in Fig. 2 C with strong increase in keratin-deficient tissue, especially in suprabasal cell layers. Bars, 20 µm. (D) Transcriptome data showing keratin mRNA expression changes in skin of Ktyl$^{-/-}$ and Ktyll$^{-/-}{}_{K8}$ compared with WTs. Note strong increase of Krt6 and Krt16 and decrease of other detectable keratin mRNAs; $n = 3$. **, $P \leq 0.01$. (E) Quantitative RT-PCR analysis of mRNAs for Krt6 in Ktyl$^{+/+}$ and Ktyl$^{-/-}$ and Krt16 and Krt17 in Ktyll$^{+/+}{}_{K8}$ and Ktyll$^{-/-}{}_{K8}$ skin of E18.5 embryos, confirming transcriptome results. Note moderate increase of Krt17 Ktyll$^{-/-}{}_{K8}$ skin. (F) Gene set enrichment analysis and gene ontology classification according to function of upregulated genes in keratin-deficient skin compared with WT at E18.5. Compared with WT, 970 and 1,179 genes were upregulated in Ktyl$^{-/-}$ and Ktyll$^{-/-}{}_{K8}$, respectively.

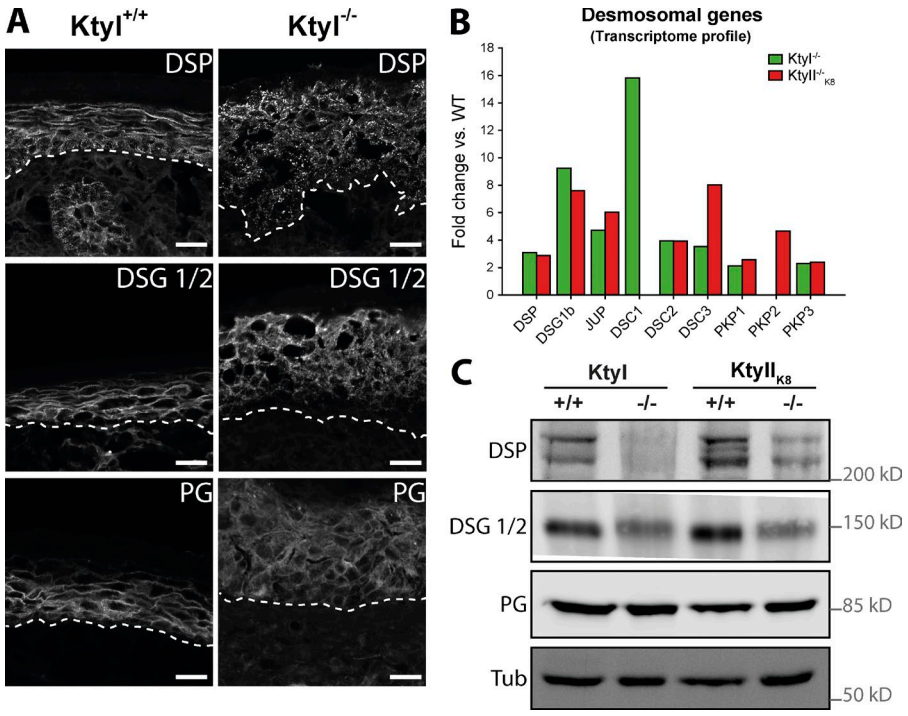

Figure S4. **Similar desmosomal defects in Ktyl$^{-/-}$ and KtyII$^{-/-}{}_{K8}$ epidermis.** (A) Immunofluorescence analysis of desmoplakin (DSP), desmogleins 1/2 (DSG1/2), and plakoglobin (PG) in WT and Ktyl$^{+/+}$ and Ktyl$^{-/-}$ epidermis at E18.5. Note cytoplasmic accumulation of DSP and DSG1/2, but not PG. The basement membrane is indicated by white dotted lines. Bars, 20 µm. (B) Transcriptional upregulation of most desmosomal genes in Ktyl$^{-/-}$ and KtyII$^{-/-}{}_{K8}$ skins based on transcriptome profiling; $n = 3$. (C) Western blotting showing decrease in DSP and DSG1/2 proteins but not of PG in skin of Ktyl$^{-/-}$ and KtyII$^{-/-}{}_{K8}$ E18.5 when compared with WT embryos.

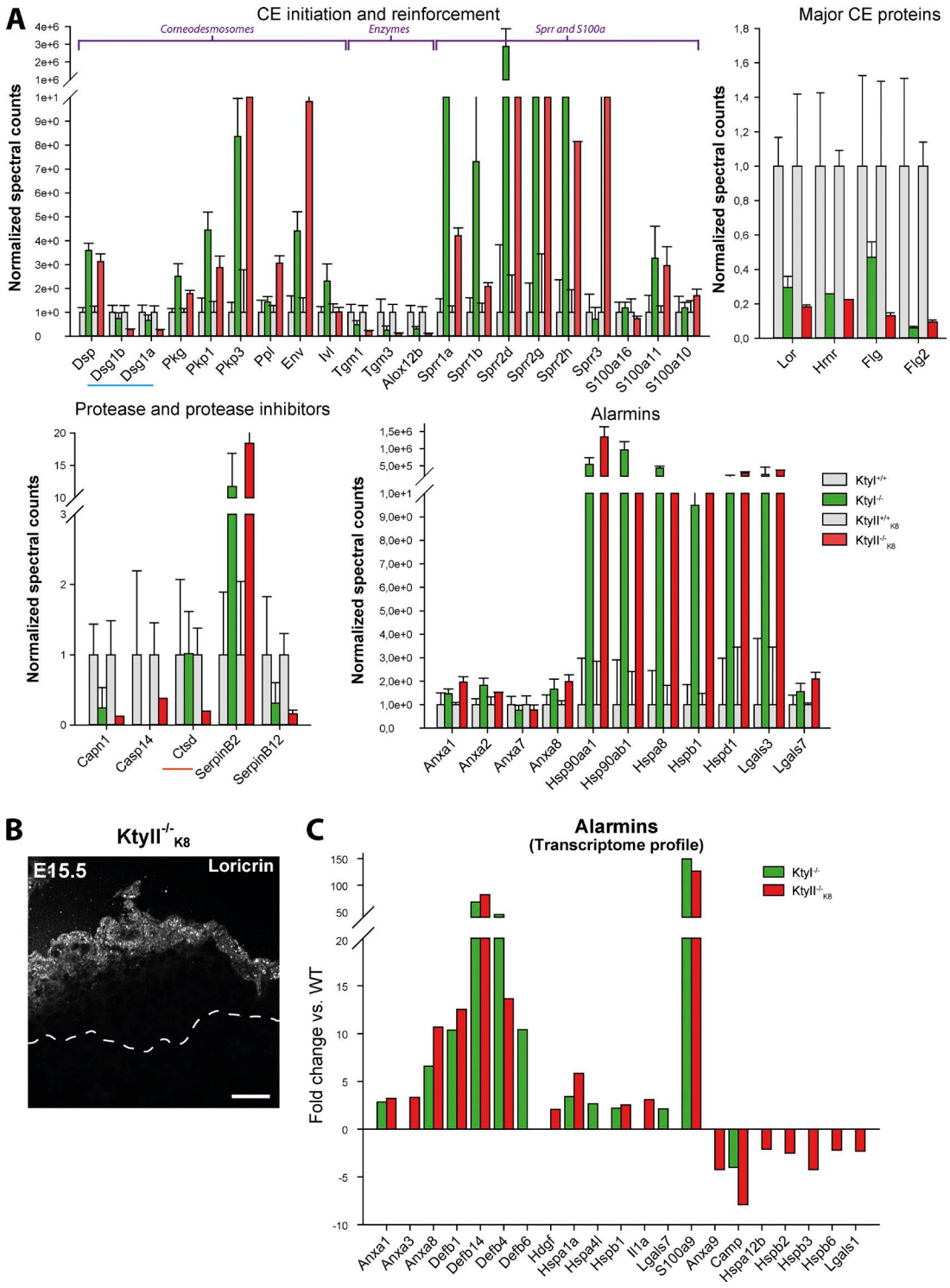

Figure S5. **Normalized CE proteome and embryonic expression of loricrin and alarmins in keratin-deficient embryos.** (A) Related to Fig. 8; normalized CE proteome profile. When not equal to 0, spectral counts of selected proteins were normalized to 1 to compare Ktyl and KtyII KO CEs together. (B) Immunofluorescence staining of loricrin in KtyII$^{-/-}{}_{K8}$ epidermis at E15.5. Bar, 20 µm. (C) Transcriptome data showing alarmin mRNA expression changes in skin of Ktyl$^{-/-}$ and KtyII$^{-/-}{}_{K8}$ compared with WT (n = 3).

Table S1. **List of primers used in the generation and analysis of KtyI mice**

Primer sequence	Product size, remarks
Forward 5′-TTTAGAGCTTGACGGGGAAAG-3′	2,452 bp; targeting of 5′ end of keratin type I cluster by PCR
Reverse 5′-TCAGGATGGCCTACAGATCAC-3′	
Forward 5′-GCTCTAGCCTCCCATTCAAAC-3′	433 bp; probes of 5′ end of keratin type II cluster targeted clones
Reverse 5′-TGACTCTCCTGCTTCTTCTGC-3′	
Forward 5′-CGCCTTTGAGTGAGCTGATAC-3′	1,780 bp; targeting of 3′ end of keratin type I cluster by PCR
Reverse 5′-GCTTAGGCAGCATCGTAAGTG-3′	
Forward 5′-GGAGAGGTCAGAGGCATTAGG-3′	497 bp; probes for 3′ end of keratin type I cluster targeted clones
Reverse 5′-AAAAAGGTTCCGTCTGGTTTG-3′	
Forward 5′-GTGGGACTCTGTAGGGACCA-3′	826 bp; *Hprt* primers to identify Cre-mediated deletion in mice
Reverse 5′-TGAACCCAGGAGGTTGAGAC-3′	
Forward 5′-AGGGCAAAGGATGTGTTACG-3′	656 bp; 3′ *hprt* probes to identify targeted and recombined loci
Reverse 5′-CCTGACCAAGGAAAGCAAAG-3′	
Forward 5′-CATTCTGCACGCTTCAAAAG-3′	616 bp; 5′ *hprt* probes to identify targeted and recombined loci
Reverse 5′-GATTCAGCCCCAGTCCATTA-3′	
Forward 5′-TCCCAATTCTCCTCATCCTC-3′	132 bp; primer used for *mK14* semiquantitative PCR
Reverse 5′-TAGTTCTTGGTGCGCAGGAC-3′	
Forward 5′-AGGAGATGACCTTGCCATCCT-3′	219 bp; primer used for *mK17* semiquantitative PCR
Reverse 5′-GGCTGATTGGCAGCGTGGAGGA-3′	
Forward 5′-GTGTTCCTACCCCCAATGTG-3′	130 bp; primer used for *GAPDH* semiquantitative PCR
Reverse 5′-AGGAGACAACCTGGTCCTCA-3′	

Table S2. **List of quantitative PCR primers used for the study**

Primer	Sequence
Nrf2	Forward 5′-CATGATGGACTTGGAGTTGC-3′ Reverse 5′-CCTCCAAAGGATGTCAATCAA-3′
Nqo1	Forward 5′-CTGGCCCATTCAGAGAAGAC-3′ Reverse 5′-GTCTGCAGCTTCCAGCTTCT-3′
Gsta3	Forward 5′-TACTTTGATGGCAGGGGAAG-3′ Reverse 5′-GCACTTGCTGGAACATCAGA-3′
HMO1	Forward 5′-CCTGGTGCAAGATACTGCCC-3′ Reverse 5′-GAAGCTGAGAGTGAGGACCCA-3′
Srxn1	Forward 5′-CGGTGCACAACGTACCAAT-3′ Reverse 5′-TTGATCCAGAGGACGTCGAT-3′
Filaggrin	Forward 5′-GCTTAAATGCATCTCCAG-3′ Reverse 5′-AGTCAGTCCTATTGCAGG-3′
Loricrin	Forward 5′-CACTCATCTTCCCTGGTGCT-3′ Reverse 5′-TCCACCAGAGGTCTTTCCAC-3′
Involucrin	Forward 5′-GGTGTACAGAAGCTTCCAAGATGTCC-3′ Reverse 5′-GGCATTGTGTAGGATGTGGAGTTGG-3′
Krt8	Forward 5′-TGGAGGGGGAGGAGAGCAG-3′ Reverse 5′-AAGGTTGGCCAGAGGATTAGG-3′
Krt16	Forward 5′-GTGAAGATCCGGGACTGGTA-3′ Reverse 5′-CATTCTCCTGGGTGGCAATA-3′
Krt17	Forward 5′-AGGAGATGACCTTGCCATCCT-3′ Reverse 5′-GGCTGATTGGCAGCGTGGAGGA-3′
Krt14	Forward 5′-TCCCAATTCTCCTCATCCTC-3′ Reverse 5′-TAGTTCTTGGTGCGCAGGAC-3′
Hornerin	Forward 5′-CGGTGTCTGGATCATCTGG-3′ Reverse 5′-CCTGGAAAGCATTGTCACTGT-3′
Krt5	Forward 5′-CGCTACCCAAACCAAGACC-3′ Reverse 5′-TCAAACCTGGGGAATGTCTC-3′
Gapdh	Forward 5′-GTGTTCCTACCCCCAATGTG-3′ Reverse 5′-AGGAGACAACCTGGTCCTCA-3′

Table S3. **List of dye and antibodies used for this study**

Targets (immunogen)	Antibodies/ fluorochromes	Hosts	Dilution		Sources	References
			Microscopy	Western blot		
Krt1 (mKrt5 625–637)	Krt1	Rabbit	1:400	1:1,000,000	Magin laboratory	–
Krt10	DE-K10	Mouse	1:150	1:10,000	Dako	M7002
Krt14 (mKrt14 471–484)	Krt14	Rabbit	1:500	1:500	Magin laboratory	–
Krt18	KS 18.04	Mouse	1:20	1:30,000	Progen	61028
Krt19 (full length)	TROMA.3	Rat	1:100	1:50,000	Baribault et al., 1994	
Krt5 (head domain)	Krt5	Guinea pig	1:300	–	Magin laboratory	Betz et al., 2006
Krt5 (hKrt5 1–16)	Krt5	Rabbit	–	1:30,000	Magin laboratory	–
Krt6 (mKrt6a 539–553; mKrt6b 548–562)	Krt6	Rabbit	1:1,000	1:300,000	Magin laboratory	–
Krt8 (full length)	TROMA.1	Rat	1:1	1:100	Baribault et al., 1994	–
Actin-F	Phalloidin-Alexa647	–	2U	–	Invitrogen	A22287
Actin-β	β-actin	Mouse	–	1:5,000	Sigma-Aldrich	A1978
Core2	CORE-2	Mouse	–	1:1,000	Abcam	ab14745
Cox1	COX1	Mouse	–	1:1,000	Invitrogen	459600
Desmoglein 1/2	DG 3.10	Mouse	1:10	1:500	Progen	61002
Desmoplakin (mDsp 2857-2875)	DP-CT	Guinea pig	1:200	1:1,000	Magin laboratory	–
E-cadherin	CDH1 Antibody (ECCD-2)	Rat	1:1,000	–	Invitrogen	13-1900
Filaggrin	Anti Filaggrin	Rabbit	1:1,000	1:10,000	Harbor Bio-Products	GTX37695
Hsp60	Hsp60	Rabbit	1:700	–	Abcam	ab46798
Integrin-β4	346-11A	Rat	1:50	–	BD	553745
Involucrin	Involucrin polyclonal antibody	Rabbit	1:500	1:200,000	Covance	PRB-140C
Keap1	D6B12	Rabbit	–	1:1,000	Cell Signaling	8047
Ki-67	SolA15	Rat	1:100	–	eBioscience	41-5698
Loricrin	AF 62	Rabbit	1:1,000	1:200,000	Covance	PRB-145 P
Ndufa9	NDUFA9	Mouse	–	1:1,000	Invitrogen	459100
Ndufv2	NDUFV2	Rabbit	–	1:200	Proteintech	15301-1-AB
Nrf2 (full length)	Nrf2	Rabbit	1:250	–	Dennis Roop	Huebner et al., 2012
Plakoglobin	PG 5.1	Mouse	1:10	1:1,000	Progen	61005
Sdha	SDHA	Mouse	–	1:1,000	Invitrogen	459200
Tubulin-α	DM1A	Mouse	–	1:12,000	Sigma-Aldrich	T9026
α-Subunit	α-subunit	Mouse	–	1:1,000	Abcam	ab110330
Nucleus	DAPI	–	1:1,000	–	Carl Roth	6335
Guinea pig IgG (H+L)	Anti–guinea pig-Cy3	Donkey	1:800	–	Dianova	706-165-148
Guinea pig IgG (H+L)	Anti–guinea pig-HRP	Goat	–	1:15,000	Dianova	106-035-003
Mouse IgG (H+L)	Anti–mouse-Cy3	Donkey	1:800	–	Dianova	715-165-151
Mouse IgG (H+L)	Anti–mouse-HRP	Goat	–	1:15,000	Dianova	115-035-003
Rabbit IgG (H+L)	Anti–rabbit-Cy3	Donkey	1:800	–	Dianova	711-165-152
Rabbit IgG (H+L)	Anti–rabbit-HRP	Goat	–	1:15,000	Dianova	111-035-003
Rat IgG (H+L)	Anti–rat-Alexa 488	Donkey	1:800	–	Dianova	712-545-153
Rat IgG (H+L)	Anti–rat-HRP	Goat	–	1:15,000	Dianova	112-035-003

–, not applicable.

References

Baribault, H., J. Penner, R.V. Iozzo, and M. Wilson-Heiner. 1994. Colorectal hyperplasia and inflammation in keratin 8-deficient FVB/N mice. *Genes Dev.* 8:2964–2973. http://dx.doi.org/10.1101/gad.8.24.2964

Betz, R.C., L. Planko, S. Eigelshoven, S. Hanneken, S.M. Pasternack, H. Bussow, K. Van Den Bogaert, J. Wenzel, M. Braun-Falco, A. Rutten, et al.. 2006. Loss-of-function mutations in the keratin 5 gene lead to Dowling-Degos disease. *Am. J. Hum. Genet.* 78:510–519. http://dx.doi.org/10.1086/500850

Huebner, A.J., D. Dai, M. Morasso, E.E. Schmidt, M. Schäfer, S. Werner, and D.R. Roop. 2012. Amniotic fluid activates the nrf2/keap1 pathway to repair an epidermal barrier defect in utero. *Dev. Cell.* 23:1238–1246. http://dx.doi.org/10.1016/j.devcel.2012.11.002